



Character of matter in holography: Spin–orbit interaction



Yunseok Seo^a, Keun-Young Kim^b, Kyung Kiu Kim^{b,c}, Sang-Jin Sin^{a,*}

^a Department of Physics, Hanyang University, Seoul 133-791, Republic of Korea

^b School of Physics and Chemistry, Gwangju Institute of Science and Technology, Gwangju 500-712, Republic of Korea

^c Department of Physics, College of Science, Yonsei University, Seoul 120-749, Republic of Korea

ARTICLE INFO

Article history:

Received 21 February 2016

Received in revised form 13 May 2016

Accepted 20 May 2016

Available online 25 May 2016

Editor: M. Cvetič

Keywords:

Holography

Diamagnetism

DC conductivity

Anomalous Hall effect

ABSTRACT

Gauge/Gravity duality as a theory of matter needs a systematic way to characterise a system. We suggest a ‘dimensional lifting’ of the least irrelevant interaction to the bulk theory. As an example, we consider the spin–orbit interaction, which causes magneto–electric interaction term. We show that its lifting is an axionic coupling. We present an exact and analytic solution describing diamagnetic response. Experimental data on annealed graphite shows a remarkable similarity to our theoretical result. We also find an analytic formulas of DC transport coefficients, according to which, the anomalous Hall coefficient interpolates between the coherent metallic regime with ρ_{xx}^2 and incoherent metallic regime with ρ_{xx} as we increase the disorder parameter β . The strength of the spin–orbit interaction also interpolates between the two scaling regimes.

© 2016 The Authors. Published by Elsevier B.V. This is an open access article under the CC BY license (<http://creativecommons.org/licenses/by/4.0/>). Funded by SCOAP³.

Overview and summary: Recently, the gauge/gravity duality [1–3] attracted much interests as a possible candidate for a reliable method to calculate strongly correlated systems. It is a local field theory in one higher dimensional space called “bulk”, with a few classical fields coupled with anti-de Sitter (AdS) gravity. Since the strong coupling in the boundary is dual to a weak coupling in the bulk, the bulk fields can be considered as local order parameters of a mean field theory in the bulk. It also provided a new mechanism for instabilities in gravity language [4] which is relevant to the superconductivity [5,6] and the metal insulator transition [7]. However, as a theory for materials, it is still in lack of one essential ingredient, a way to distinguish one matter from the others. Although electron–electron interaction is traded for the gravity in the bulk, we still need to specify lattice–electron interactions to characterise the system. Without it, we would not know what system we are working for.

Naively one may try to introduce realistic lattice at the boundary to mimic the reality. However, its effects are mostly irrelevant in the infrared (IR) limit. In strong coupling limit where no quasiparticle exists, no Fermi surface (FS) exists either. Actually in the absence of the FS, it is almost impossible to write down any relevant *interaction* term in a local field theory in higher than

1+1 dimension.¹ Therefore non-local effect may be essential for any interesting physics in strongly interacting system. One interesting aspect of a holographic theory is that any local interaction in the bulk has non-local effect in the boundary [9]. Usually one characterises a many body system in continuum limit by a few interaction terms rather than the detail of structure. Therefore, to characterise a system in holographic theory, what we want to suggest is the dimensional-lifting, by which we mean promoting the “system characterising interaction” of the boundary theory to a term in the bulk theory using the covariant form of the interaction.

One may wonder what the gravity dual of the Maxwell theory is. In condensed matter, there are two components of electromagnetic interaction. One is electron–electron interaction and the other is lattice–electron interaction. While the main difficulty is coming from the former, system is characterised by the latter. Working hypothesis is that the electron–electron interaction is taken care of by working in asymptotic AdS gravity. Our purpose is to include the electron–lattice interaction in this holographic scheme, which is possible for two reasons. First, in any boundary system with a conserved global $U(1)$ charge, we have a bulk Maxwell theory, which can accommodate usual electromagnetic field as a probe or an external source. It was used to build

* Corresponding author.

E-mail addresses: yseo@hanyang.ac.kr (Y. Seo), fortoe@gist.ac.kr (K.-Y. Kim), kimkyungkiu@gmail.com (K.K. Kim), sangjin.sin@gmail.com (S.-J. Sin).

¹ See however ref. [8] for semi-holographic approach based on IR AdS2 and its virtual CFT_2 , which is different from ours.

the holographic version of superconductivity mentioned above and also to calculate electric/thermal transport coefficients [10–13]. Second, we can use a relativistic theory for a non-relativistic system. The relativistic invariance highly constrains the possible form of extension of interaction. A practical way to proceed is to turn on the interaction one by one for technical simplicity. The covariant form of the interaction is either scalar or top form. The former is trivially lifted to higher dimension, e.g., $F_{\mu\nu}M^{\mu\nu}$ can be used in any dimension. Now suppose the top form of the boundary theory is F_d and the bulk theory already contains scalar operator φ and one form ω_1 . Then we have essentially two choices: φdF_d and $\omega_1 \wedge F_d$ to avoid the total derivative term.

To discuss the idea in more specific context, we consider the spin-orbit interaction in 2+1 dimensional systems. It creates lots of interesting phenomena including topological insulators and Weyl semi-metal [14–18] by changing band structures, which in turn causes magneto-electric phenomena [19,20] like anomalous Hall effect. Naively, introducing the spin-orbit interaction involve fermions.² However, we can integrate out the massive fermions, thereby avoid dealing with fermions in our theory. Notice that in the absence of Fermi sea as in our strong coupling problem, fermions can be considered to be massive. It is well known that the fermions integrated out leave the Chern–Simons term $A \wedge F$ [21,22], which can be lifted to 4 dimension as $F \wedge F \sim E \cdot B$.³ Since it is a total derivative by itself, we have to couple it with an appropriate scalar operator to have a non-trivial dynamical effect. In this paper, we choose it to be the kinetic energy term of the axion scalar fields χ_I . That is our interaction term is $q_\chi \sum_{I=1,2} (\partial\chi_I)^2 F \wedge F$, where χ_I was introduced to provide some disorder giving momentum dissipation [32]. Notice that this term is odd in time reversal, which is appropriate for the case where magnetisation is non-trivial.⁴

Since we want to have finite temperature, chemical potential, magnetic fields, and finite DC conductivity, the system should contain metric, gauge fields and axion scalar fields ($g_{\mu\nu}, A_\mu, \chi_I$) as the minimal ingredients in the bulk. So we have to start with the Einstein–Maxwell–axion system. We have found an exact analytic solution of such a non-trivially coupled system with a new interaction term, consequently yielding an explicit and analytic result for the DC conductivity using recent technology [10–12]. While the Hall effect is obviously connected to our system from the construction, the fully back reacted system shows diamagnetic response. This is because we examined metallic state at finite temperature and did not include spin degrees of freedom explicitly. Finally, we comment on the relevance of our result to experimental data. In [33], it was reported that graphite, once annealed to wash out the ferromagnetic behaviour, shows a non-linear diamagnetic response which is very similar to our analytic result. Also it turns out that our analytic conductivity formulas reproduce the experimental data on the scaling relation between the non-linear anomalous Hall coefficients and the longitudinal resistivity. I.e. the non-linear anomalous Hall coefficients interpolate between the linear and

quadratic dependence on the longitudinal resistivity. Considering that we added just one interaction term, these are unexpectedly rich consequences.

The model and background solution: With motivations described above, we start from the Einstein–Maxwell–axion action with the Chern–Simons interaction

$$2\kappa^2 S = \int d^4x \sqrt{-g} \left\{ R + \frac{6}{L^2} - \frac{1}{4} F^2 - \sum_{I=1,2} \frac{1}{2} (\partial\chi_I)^2 \right\} - \frac{1}{16} \int q_\chi (\partial\chi_I)^2 F \wedge F + S_c, \quad (1)$$

where q_χ is a coupling, and $\kappa^2 = 8\pi G$ and L is the AdS radius and we set $2\kappa^2 = L = 1$. S_c is the counter term which is necessary to make the action finite. Explicit form of S_c is written in (25) at the end of this paper. The axion (χ_I) which is linear in $\{x, y\}$ direction breaks translational symmetry and hence gives an effect of momentum dissipation [32]. Instanton density coupled with the axion can generate magneto-electric property: if we add charge, non-trivial magnetisation is generated. The equations of motion are rather long so we wrote it in (26) at the end.

As ansatz to solutions, we use the following form

$$A = a(r)dt + \frac{1}{2}H(xdy - ydx), \quad (2)$$

$$\chi_1 = \beta x, \quad \chi_2 = \beta y,$$

with the metric ansatz

$$ds^2 = -U(r)dt^2 + \frac{dr^2}{U(r)} + r^2(dx^2 + dy^2). \quad (3)$$

From the equations of motion, we found exact solution

$$U(r) = r^2 - \frac{\beta^2}{2} - \frac{m_0}{r} + \frac{q^2 + H^2}{4r^2} + \frac{\beta^4 H^2 q_\chi^2}{20r^6} - \frac{\beta^2 H q q_\chi}{6r^4}, \quad (4)$$

$$a(r) = \mu - \frac{q}{r} + \frac{\beta^2 H q q_\chi}{3r^3},$$

where μ is a free parameter interpreted as the chemical potential and q and m_0 are determined by the condition $A_t(r_0) = U(r_0) = 0$ at the black hole horizon (r_0). q is the conserved $U(1)$ charge interpreted as a number density at the boundary system. m_0 turns out to be half of the energy density (9) and β is related to momentum relaxation rate

$$q = r_0 \mu + \frac{1}{3} \theta H \quad \text{with} \quad \theta = \frac{\beta^2 q_\chi}{r_0}, \quad (5)$$

$$m_0 = r_0^3 + \frac{r_0^2 \mu^2 + H^2 - 2\beta^2 r_0^2}{4r_0} + \frac{\theta^2 H^2}{45r_0}.$$

The solution (4) reproduces the dyonic black hole solution with momentum relaxation [12] when q_χ vanishes.

Diamagnetic response: The thermodynamic potential density \mathcal{W} in the boundary theory is computed by the Euclidean on-shell action S^E of (25): $S^E \equiv \mathcal{V}_2 \mathcal{W} / T$, $\mathcal{V}_2 = \int dx dy$ using the solutions (2)–(3)

$$\mathcal{W} = -r_0^3 - \frac{1}{4r_0} (\mu^2 r_0^2 + 2\beta^2 r_0^2 - 3H^2) + \frac{2}{3} \mu \theta H + \frac{7}{45r_0} \theta^2 H^2. \quad (6)$$

The system temperature T is identified with the Hawking temperature of the black hole,

$$T = \frac{3}{4\pi} r_0 - \frac{1}{16\pi r_0^3} \left((q - \theta H)^2 + H^2 + 2r_0^2 \beta^2 \right), \quad (7)$$

² The Chern–Simons term is derived from a minimal interaction $\bar{\psi} \gamma^\mu \psi A_\mu$. If we take non-relativistic limit first, the interaction Lagrangian is $L_{int} = \bar{\mu} \cdot \vec{B}$ in the electron at rest frame, which becomes $\bar{\psi} \gamma^{\mu\nu} \psi F_{\mu\nu}$ in covariant form that is valid in any frame. When we include fermions explicitly, we have to take into account this issue.

³ Previously the Chern–Simons term in the bulk and its higher dimensional analogue were extensively considered in holography to discuss the chiral effects or instability to the inhomogeneous phases [23–31].

⁴ In order to handle time reversal invariant case, one can consider $q_\chi \sum_{I=1,2} d\chi_I \wedge A \wedge F \sim q_\chi \sum_{I=1,2} \chi_I F \wedge F$. One can also consider the possibility that q_χ contains an Ising spin variable ± 1 which is odd under time reversal. In this paper we focus on the time reversal breaking case to consider non-zero magnetisation.

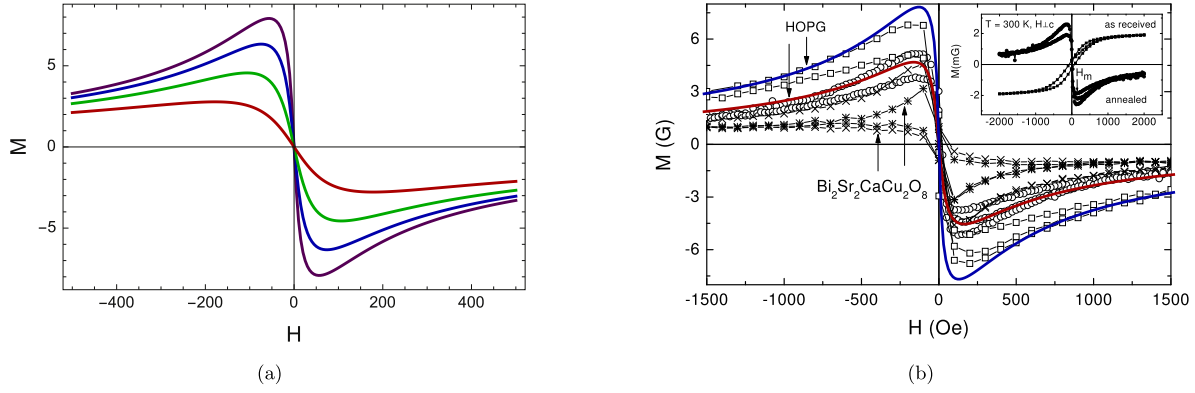


Fig. 1. (a) The external magnetic field dependences of the magnetisation at $T = 1$ (purple), $T = 1.2$ (blue), $T = 1.5$ (green) and $T = 2$ (red) with $q_\chi = 10$, $\beta = 2.2$, $\mu = 0$. (b) Theory curve compared with experimental data of annealed highly oriented pyrolytic graphite (HOPG) sample for $T = 150$ K (rectangle) and $T = 300$ K (circle) in [33]. For comparison, the blue and red curves obtained by our formula (14) are added. The red one is for $T = 1$, $\beta = 2$ and the blue one is for $T = 0.8$, $\beta = 2.2$, $q_\chi = 10$ and $\mu = 0$ for both cases. (For interpretation of the references to colour in this figure legend, the reader is referred to the web version of this article.)

and the entropy density is given by the area of the horizon

$$s = 4\pi r_0^2. \quad (8)$$

We have numerically checked that the entropy is a monotonically increasing function of temperature for the parameters analysed in this paper. The energy density ε is one point function of the boundary energy momentum tensor T_{00} , which is holographically encoded in the metric (5):

$$\varepsilon = \langle T_{00} \rangle = 2m_0. \quad (9)$$

It is remarkable that the complicated expression of the thermodynamic potential density (6) gives a simple thermodynamic relation

$$\mathcal{W} = \varepsilon - sT - \mu q, \quad (10)$$

with energy, temperature and entropy given by (7), (8) and (9). The variation of the potential density (6) boils down to

$$\delta\mathcal{W} = -\tilde{M}\delta H - s\delta T - q\delta\mu, \quad (11)$$

where

$$\tilde{M} \equiv \frac{1}{r_0} \left(-H + \frac{1}{3}\theta q - \frac{1}{5}\theta^2 H \right). \quad (12)$$

Notice that the (10) and (11) implies the first law of thermodynamics;

$$\delta\varepsilon = -\tilde{M}\delta H + T\delta s + \mu\delta q. \quad (13)$$

Two important remarks are in order: First, H is interpreted as an externally applied field, although it is a fully back reacted object in the bulk. H is the magnetic field generated by free current, not the magnetic induction which is usually denoted by B . This is because we did not encode any spin dynamics in the bulk and we do not have fully dynamical gauge fields at the boundary. The Maxwell fields at the boundary enter as an external source or as a weak probe field.

Second, \tilde{M} has dimension 1 and describes a genuine 2+1 dimensional system. Therefore, it can not be identified as the magnetisation M of a physical system which is a 2 dimensional array in 3 spatial dimension. Furthermore, since \tilde{M} and H are different in mass dimension, they cannot be added to form magnetic induction B . The magnetic field H and magnetisation M are those of spatial 3 dimension, therefore both H and M should have the same mass dimension 2. If we just multiply \tilde{M} by r_0 , a mass dimension 1 parameter which is a constant for adiabatic processes, we would get $B = H + M = 0$ for $q_\chi = 0$. It means that the dyonic black hole

exhibits the Meisner effect, which is not physical. The problem can be traced to the fact that after we scale ε by r_0 to balance the dimension of M and H , the free energy contains $H^2/2$, which is the field energy of magnetic field applied on vacuum. When we calculate the magnetisation by taking its derivative, we should subtract it from the free energy as suggested by Landau and Lifshitz in section 32 of ref. [34]. Therefore, we calculate the magnetisation from $F \equiv r_0\varepsilon - \frac{1}{2}H^2$:

$$M = -\left. \frac{\partial F}{\partial H} \right|_{\text{fixed } r_0, q} = \theta q/3 - \theta^2 H/5. \quad (14)$$

Both terms here are the consequences of the axionic coupling.

The first term is the magnetisation at $H = 0$, which will be denoted by M_0 . It is proportional to the charge of the system and gives ferromagnetism. More explicitly,

$$M_0 = \frac{1}{3}\theta q = \frac{\mu\beta^2 q_\chi}{3r_0}, \quad (15)$$

with $r_0 = (4\pi T + \sqrt{16\pi^2 T^2 + 3(\mu^2 + 2\beta^2)})/6$ at $H = 0$. For given μ , β and q_χ , M_0 has the maximum value at zero temperature and decreases as $1/T$ for large temperature. In the coherent metallic regime [35] $\beta/\mu \ll 1$, $M_0 \sim \beta^2 q_\chi$. The second term in (14) represents the back reaction of the system to the external magnetic field and gives diamagnetism.

We want to analyse the magnetisation as a function of the magnetic field with the other parameters fixed. Notice that, at fix temperature, r_0 has to be computed from (7). In Fig. 1(a), we draw the magnetic field dependence of the magnetisation at different temperatures for $\mu = 0$, $q_\chi = 10$, and $\beta = 2$. The magnetisation seems to be saturated for large magnetic field and the magnetic susceptibility is decreasing function of temperature. Our results are very similar to the graphite data in Fig. 1(b) [33]. Here, in addition to experimental data, we added the blue and red curves using our formula (14) for comparison, where the red one is for $T = 1$, $\beta = 2$ and the blue one is for $T = 0.8$, $\beta = 2.2$, $q_\chi = 10$ and $\mu = 0$ for both cases.

DC transport coefficients: Recently, a systematic way to compute the DC transport coefficients has been developed in [11,12,36] by which we can compute the longitudinal and transverse electric and thermoelectric conductivities. Here we write only result.

$$\begin{aligned}\sigma_{xx} &= \frac{(\mathcal{F} - H^2)(\mathcal{F} + \mathcal{G}^2)}{(\mathcal{F}^2 + H^2\mathcal{G}^2)}, \\ \sigma_{xy} &= \frac{HG(2\mathcal{F} + \mathcal{G}^2 - H^2) + \theta(\mathcal{F}^2 + H^2\mathcal{G}^2)}{(\mathcal{F}^2 + H^2\mathcal{G}^2)}, \\ \alpha_{xx} &= \frac{s\mathcal{G}(\mathcal{F} - H^2)}{\mathcal{F}^2 + H^2\mathcal{G}^2}, \quad \alpha_{xy} = \frac{sH(\mathcal{F} + \mathcal{G}^2)}{\mathcal{F}^2 + H^2\mathcal{G}^2} - \frac{H}{r_0},\end{aligned}\quad (16)$$

where

$$\begin{aligned}\mathcal{F} &= r_0^2\beta^2 + H^2(1 + \theta^2) - \theta qH, \\ \mathcal{G} &= q - \theta H, \quad s = 4\pi r_0^2.\end{aligned}\quad (17)$$

We gave some details at the end. We check two limits: i) for $\beta = 0$, the DC conductivities (16) become $\sigma_{xx} = 0$, $\sigma_{xy} = q/H$, $\alpha_{xx} = 0$ and $\alpha_{xy} = s/H$, which agrees with [37]; ii) for $q_\chi = 0$ (16) reproduces the result obtained in [12,36].

At finite β and finite q_χ but with $H = 0$ the electric conductivities reduce to:

$$\sigma_{xx} = 1 + \frac{\mu^2}{\beta^2}, \quad \sigma_{xy} = \theta = \frac{3M_0}{q}.\quad (18)$$

Notice that σ_{xx} is a known result [32], but, interestingly, σ_{xy} is non-zero even when $H = 0$. This phenomena is related to *anomalous* Hall effect, which will be discussed next. It is the result of the axion coupling we introduced, which gives a ferromagnetism with the magnetisation M_0 (15).

Anomalous Hall effect: In ferromagnetic conductor, the Hall effect is about 10 times bigger than in non-magnetic material. This stronger Hall effect in ferromagnetic conductor is known as the anomalous Hall (AH) effect [38,39]. The precise mechanism for AH effect has a century-long history of debates [38]. Three mechanisms have been suggested: i) intrinsic one due to anomalous velocity, ii) side jump, iii) skew scattering. Mechanism i) was suggested in 1950's by Karpulus and Luttinger. In modern days, the anomalous velocity is understood by the Berry phase ($\mathbf{v}_a = \frac{e}{\hbar} \mathbf{E} \times \mathbf{b}_{\text{Berry}}$). Side jump mechanism is suggested by Berger in ref. [40] where he showed that the electron velocity is deflected in opposite directions by the opposite electric fields experienced upon approaching and leaving an impurity. The skew scattering was suggested by Smit in [41,42] where he noticed that asymmetric scattering from impurities is caused by the spin-orbit interaction. The fundamental interaction underlying all these three is the spin-orbit interaction.

It has been known that there is a power law relationship between the anomalous part (R_S) of the Hall resistivity (ρ_{yx}) and the longitudinal resistivity (ρ_{xx}):

$$R_S \sim \rho_{xx}^\alpha, \quad (19)$$

with the anomalous Hall coefficient, R_S , defined by the relation

$$\rho_{yx} = R_H H + R_S M, \quad (20)$$

where R_H is the usual Hall coefficient. The power α had been computed for three scenarios to give $\alpha = 2$ for i), ii) and $\alpha = 1$ for iii).

From (14) and (18) our model describes a ferromagnetic conductor, therefore it will be interesting to study AH effect. The resistivity matrix (ρ) can be computed by inverting the conductivity matrix (σ) in (16) i.e. $\rho = \sigma^{-1}$. R_S is identified by ρ_{yx} at $H = 0$:

$$\rho_{yx}|_{H=0} = \frac{\theta}{\theta^2 + (1 + \mu^2/\beta^2)^2} = R_S M_0. \quad (21)$$

Since $M_0 = \frac{1}{3}q\theta$, anomalous Hall coefficient is given by

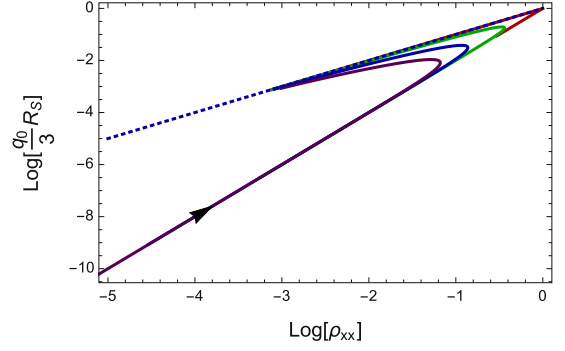


Fig. 2. Relation between ρ_{xx} and $\frac{3}{2}R_S$ ($q_0 \equiv \mu r_0$) at fixed $q_\chi = 1$ with $\mu/T = 0.1$ (red), 2 (green), 5 (blue) and 10 (purple) in log-log plot. The arrow represents the direction of increasing β/μ . $R_S \sim \rho_{xx}^2$ in small β/μ and $R_S \sim \rho_{xx}$ in large β/μ regime. (For interpretation of the references to colour in this figure legend, the reader is referred to the web version of this article.)

$$R_S = \frac{3}{r_0\mu} \frac{1}{\theta^2 + (1 + \mu^2/\beta^2)^2}. \quad (22)$$

The longitudinal resistivity at $H = 0$ reads

$$\rho_{xx} = \frac{1 + \mu^2/\beta^2}{\theta^2 + (1 + \mu^2/\beta^2)^2}. \quad (23)$$

The scaling behaviours can be read easily for two limits:

$$R_S \sim \rho_{xx}^2, \quad \text{or} \quad R_S \sim \rho_{xx}, \quad (24)$$

depending on $\beta/\mu \ll 1$ or $\beta/\mu \gg 1$. The same scaling relations hold for $\theta \ll 1$ or $\theta \gg 1$. For general value of β/μ , the scaling behaviour is shown in Fig. 2 as the slope. In the figure, the arrow represents the directions of increasing disorder parameter β , and $\mu/T = 0.1$ (red), 2 (green), 5 (blue) and 10 (purple). Notice the transition from $\alpha = 2$ to $\alpha = 1$ is sharper for larger temperature. Notice also that $\alpha = 2$ for small β/μ whatever is the spin-orbit interaction strength θ .

In ref. [35], material with $\beta/\mu \ll 1$ was identified as a coherent metal of which optical conductivity has a well defined Drude peak as if it had quasiparticles. For $\beta/\mu \gg 1$, the system behaves as an incoherent metal without a Drude peak. Interestingly, such electrically classified coherent/incoherent metal also shows AH property with the characteristic power $\alpha = 2, 1$. This is consistent with the interpretation of β as impurity density since large β would have much extrinsic disorder effects. Notice that we have two scaling regimes in one model with interpolating parameters given by the disorder parameter β or spin-orbit coupling strength θ , while in conventional method different scalings are associated with different mechanisms. The fact that all three mechanisms are originated from spin-orbit interaction is reflected to our result which is a consequence of adding just one interaction term representing spin-orbit coupling.

Method: DC conductivities from black hole horizon

Here we explain how to obtain the DC conductivities (16). The action with counter terms are given by

$$\begin{aligned}2\kappa^2 S &= \int_{\mathcal{M}} d^4x \sqrt{-g} \left\{ R + \frac{6}{L^2} - \frac{1}{4}F^2 - \sum_{l=1,2} \frac{1}{2}(\partial\chi_l)^2 \right\} \\ &\quad - \frac{1}{16} \int_{\mathcal{M}} q_\chi (\partial\chi_l)^2 F \wedge F + S_c, \\ S_c &= - \int_{\partial\mathcal{M}} d^3x \sqrt{-\gamma} \left(2K + \frac{4}{L} + R[\gamma] - \sum_{l=1,2} \frac{L}{2} \nabla\chi_l \cdot \nabla\chi_l \right).\end{aligned}\quad (25)$$

The equations of motion are

$$\begin{aligned} \nabla^2 \chi_I + \frac{q\chi}{8} \nabla_M \left(\frac{1}{\sqrt{-g}} \epsilon^{PQRS} F_{PQ} F_{RS} \nabla^M \chi_I \right) &= 0, \\ \nabla_M F^{MN} + \frac{q\chi}{4} \nabla_M \left((\partial \chi_I)^2 \frac{1}{\sqrt{-g}} \epsilon^{MNPQ} F_{PQ} \right) &= 0, \\ R_{MN} - \frac{1}{2} g_{MN} \left(R + 6 - \frac{1}{4} F^2 - \frac{1}{2} (\partial \chi_I)^2 \right) \\ &\quad - \frac{1}{2} F_{MP} F_N{}^P - \frac{1}{2} \partial_M \chi_I \partial_N \chi_I \\ &\quad - \frac{q\chi}{16} \partial_M \chi_I \partial_N \chi_I \frac{1}{\sqrt{-g}} \epsilon^{PQRS} F_{PQ} F_{RS} = 0, \end{aligned} \quad (26)$$

where $\epsilon^{0123} = \epsilon^{txyr} = 1$.

Once we get a background solution of these equations, we can compute the DC transport coefficients from the black hole horizon data. Let us start by defining a useful quantity:

$$\mathcal{F}^{MN} \equiv \sqrt{-g} F^{MN} + \frac{q\chi}{4} (\partial \chi)^2 \epsilon^{MNPQ} F_{PQ}. \quad (27)$$

Then the Maxwell equation and the boundary current can be written as

$$\partial_M \mathcal{F}^{MN} = 0, \quad J_{tot}^\mu = \lim_{r \rightarrow \infty} \mathcal{F}^{\mu r}. \quad (28)$$

If we assume all fields depend on t and r , one can obtain another expression for the total boundary current using the Maxwell equation

$$J_{tot}^\mu = \lim_{r \rightarrow r_0} \mathcal{F}^{\mu r} + \int_{r_0}^{\infty} dr \partial_t \mathcal{F}^{t\mu}. \quad (29)$$

Now we want to consider fluctuations corresponding to the boundary DC electric field E_i and the DC temperature gradient $\zeta_i = \frac{v_i}{T}$. Following [11], we may consider fluctuations around the background as follows:

$$\begin{aligned} \delta A_i &= -(E_i - \zeta_i a(r)) t + \delta a_i(r), \\ \delta g_{ti} &= -U(r) \zeta_i t + r^2 \delta h_{ti}, \\ \delta g_{ri} &= r^2 \delta h_{ri}, \\ \delta \chi_i &= \delta \chi_i(r). \end{aligned} \quad (30)$$

In the linear level the time dependent part of the equations of motion drops out by the above choice of fluctuations. Thus these fluctuations are stable static fluctuations to the DC sources, (E_i, ζ_i) .

To be a physical fluctuation in the black hole background, the fluctuation should satisfy the in-falling boundary condition as it approaches the horizon. This condition can be described in terms of the Eddington–Finkelstein coordinates $v = t + \frac{1}{4\pi T} \ln(r - r_0)$, and the in-falling fluctuation should depend on v near horizon. Therefore, the regularity at the horizon implies

$$\begin{aligned} \delta h_{ti} &\sim -\frac{\zeta_i}{4\pi T} \log(r - r_0) \frac{U(r)}{r^2} + h_{ti}^{(0)} + \mathcal{O}((r - r_0)), \\ \delta h_{ri} &\sim \frac{\mathbb{H}_{ri}}{r^2 U(r)} + h_{ri}^{(0)} + \mathcal{O}((r - r_0)), \\ \delta a_i &\sim -\frac{E_i - \zeta_i a(r)}{4\pi T} \log(r - r_0) + a_i^{(0)} + \mathcal{O}((r - r_0)), \\ \delta \chi_i &\sim \delta \chi_i^{(0)} + \mathcal{O}((r - r_0)). \end{aligned} \quad (31)$$

By expanding (r, i) component and (t, i) component of the Einstein equations, it turns out that $\mathbb{H}_{ri} = r_0^2 h_{ti}^{(0)}$ and $h_{ti}^{(0)}$ can be determined.⁵

Now we are ready to consider the total current (29) in the linear level. The current can be calculated by plugging (4) and the fluctuation (30). Firstly, the second part is

$$\begin{aligned} \int_{r_0}^{\infty} dr \partial_t \mathcal{F}^{ti} &= \frac{\epsilon_{ij}}{r_0} \left(-H + \frac{1}{3} \theta q - \frac{1}{5} \theta^2 H \right) \zeta_j \\ &= \frac{\epsilon_{ij}}{r_0} (-H + M) \zeta_j. \end{aligned} \quad (32)$$

The second term is the contribution of the magnetisation current J_{mag} [43]. Thus the relevant part of the current is the first term, which can be written in terms of the horizon data:

$$\begin{aligned} J^\mu &= \lim_{r \rightarrow r_0} \mathcal{F}^{\mu r} \\ &= E_i - (q - \theta H) h_{ti}^{(0)} - \frac{H}{r_0^2} \epsilon_{ij} \mathbb{H}_{rj} + \epsilon_{ij} \theta E_j - \epsilon_{ij} \frac{H}{r_0} \zeta_j. \end{aligned} \quad (33)$$

Finally, the expressions $h_{ti}^{(0)}$ and \mathbb{H}_{ri} obtained from the Einstein equation give us the electric conductivities and the thermoelectric coefficients (16) using formula $\sigma_{ij} = \frac{\partial J^i}{\partial E_j}$ and $\alpha_{ij} = \frac{\partial J^i}{\partial \zeta_j}$. The details of $h_{ti}^{(0)}$ and \mathbb{H}_{ri} will be given in a longer version of this work.

Summary and discussion: We view the holographic principle as a set of axioms to calculate strongly interacting systems. For reader's convenience we first list them below [9].

1. For a strongly interacting system with conformal symmetry at UV, there is a dual gravity with asymptotic AdS boundary. Non-AdS geometry may be regarded as an IR part of an asymptotic AdS geometry.
2. To calculate the correlation function of an operator \mathcal{O}_Δ with dimension Δ and spin p , we introduce a source field $\phi_0(x)$ with spin p and dimension Δ . Extend $\phi_0(x)$ into one higher dimensional space $\phi(x, r)$ such that $\phi(x, r = \infty) \sim \phi_0(x)/r^{d-2p-\Delta}$. Identify the generating function of conformal field theory $Z[\phi_0]$ with that of gravitational system $\exp(-S[\phi_0])$.
3. For a global symmetry at the bulk, we have a local gauge symmetry at the boundary.
4. For Euclidean Green functions, Dirichlet boundary value at infinity is enough. For causal green function, assign the boundary condition (BC) at the IR region in addition to the Dirichlet BC at the infinity.
5. Temperature and chemical potential are provided by regularity of metric, gauge fields at the horizon or its replacing IR geometry.
6. Characterise the system by lifting the least irrelevant interactions at the boundary to the bulk. For strongly correlated electron system, the electron–electron interaction is counted by the gravity, but electron–lattice interactions should be taken into account explicitly. The gauge field dual to the conserved $U(1)$ current can have interaction terms to take care of electron–lattice interactions.

The last item is what we added in this paper. In this paper, we considered the magneto–electric phenomena induced by the spin–orbit coupling interaction as an example of dimensional lifting in holographic theory. When electron spins are correlated, adding charge carrier changes the magnetic property as well as the charge

⁵ Since the expression is lengthy but not very illuminating we don't present here.

transport. In effective field theory approach, such electric–magnetic effect can be implied by adding the Chern–Simons term $\sim A \wedge F$ in 2+1 dimension. It act as a crossing source of electricity and magnetism. With such a term, the system can pick up a magnetic source when we provide electric charge and vice versa.

We work at finite temperature, chemical potential, and magnetic fields. The metric, gauge and axion fields ($g_{\mu\nu}, A_\mu, \chi_I$) are playing the role of coupled order parameters. We have found the exact and analytic solution of such a complicated coupled system with a non-trivial interaction, which made it possible to get an explicit and analytic DC conductivity formulas.

When we split the current into orbital and magnetisation parts, it depends on the definition of the magnetisation, namely, whether we use M or \tilde{M} . The electric conductivity does not change but thermo-electric conductivity changes. The α for M and that for \tilde{M} are related in simple manner: σ_{ij} and α_{xx} are not changed while $\alpha_{xy}^M = \alpha_{xy}^{\tilde{M}} - H/r_0$. It turns out that Onsager relations are valid in both cases, $\alpha = \tilde{\alpha}$, a remarkable fact.

Our results on the Hall resistivity shows a non-linear diamagnetic response is similar to that of graphite system and also to high T_c superconductor $\text{Bi}_2\text{Sr}_2\text{CaCu}_2\text{O}_8$. Also we have shown that the anomalous Hall coefficients in our model interpolate between the linear and quadratic regime on the resistivity dependence as a function of disorder parameter and spin-orbit interaction coupling. It is particularly interesting to see that electrical coherent/incoherent metal has magnetic behaviour with quadratic/linear resistivity dependence. Experimentally diverse materials were studied. Some shows α near 2 and the other 1, sometimes old and new data crashes. So, detailed data mining is postponed to future investigation.

Our model does not include paramagnetic behaviour because we integrated out fermion and therefore spin degrees of freedom is not included explicitly. Also we could have chosen the scalar field χ itself instead of its kinetic term as a scalar partner of $F \wedge F$ term. We will report on these issues elsewhere.

Acknowledgements

The authors want to thank Junghoon Han for suggesting to look graphite data for diamagnetism. SS appreciates discussions with Yunkyung Bang, Yongbaek Kim, Kwon Park and especially Kiseok Kim on many related issues. YS want to thank KIAS for the financial support during his visit. The work of SS and YS was supported by Mid-career Researcher Program through the National Research Foundation of Korea (NRF) grant No. NRF-2013R1A2A2A05004846. The work of KKY and KKK was supported by Basic Science Research Program through the National Research Foundation of Korea (NRF) funded by the Ministry of Science, ICT and Future Planning (NRF-2014R1A1A1003220) and the 2015 GIST Grant for the FARE Project (Further Advancement of Research and Education at GIST College).

References

- [1] Juan Martin Maldacena, The large N limit of superconformal field theories and supergravity, *Int. J. Theor. Phys.* 38 (1999) 1113–1133.
- [2] Edward Witten, Anti-de Sitter space and holography, *Adv. Theor. Math. Phys.* 2 (1998) 253–291.
- [3] S.S. Gubser, Igor R. Klebanov, Alexander M. Polyakov, Gauge theory correlators from noncritical string theory, *Phys. Lett. B* 428 (1998) 105–114.
- [4] Steven S. Gubser, Breaking an Abelian gauge symmetry near a black hole horizon, *Phys. Rev. D* 78 (2008) 065034.
- [5] Sean A. Hartnoll, Christopher P. Herzog, Gary T. Horowitz, Holographic superconductors, *J. High Energy Phys.* 12 (2008) 015.
- [6] Frederik Denef, Sean A. Hartnoll, Landscape of superconducting membranes, *Phys. Rev. D* 79 (12) (2009) 126008.
- [7] Aristomenis Donos, Sean A. Hartnoll, Interaction-driven localization in holography, *Nat. Phys.* 9 (2013) 649–655.
- [8] Thomas Faulkner, Joseph Polchinski, Semi-holographic Fermi liquids, *J. High Energy Phys.* 06 (2011) 012.
- [9] Sean A. Hartnoll, Horizons, holography and condensed matter (2011).
- [10] Aristomenis Donos, Jerome P. Gauntlett, Novel metals and insulators from holography, *J. High Energy Phys.* 06 (2014) 007.
- [11] Aristomenis Donos, Jerome P. Gauntlett, Thermoelectric DC conductivities from black hole horizons, *J. High Energy Phys.* 1411 (2014) 081.
- [12] Keun-Young Kim, Kyung Kiu Kim, Yunseok Seo, Sang-Jin Sin, Thermoelectric conductivities at finite magnetic field and the Nernst effect (2015).
- [13] Xian-Hui Ge, Yi Ling, Chao Niu, Sang-Jin Sin, Thermoelectric conductivities, shear viscosity, and stability in an anisotropic linear axion model, *Phys. Rev. D* 92 (10) (2015) 106005.
- [14] M. Zahid Hasan, Charles L. Kane, Colloquium: topological insulators, *Rev. Mod. Phys.* 82 (4) (2010) 3045.
- [15] Xiao-Liang Qi, Shou-Cheng Zhang, Topological insulators and superconductors, *Rev. Mod. Phys.* 83 (4) (2011) 1057.
- [16] Liang Fu, Charles L. Kane, Topological insulators with inversion symmetry, *Phys. Rev. E* 76 (4) (2007) 045302.
- [17] Haijun Zhang, Chao-Xing Liu, Xiao-Liang Qi, Xi Dai, Zhong Fang, Shou-Cheng Zhang, Topological insulators in Bi_2Se_3 , Bi_2Te_3 and Sb_2Te_3 with a single Dirac cone on the surface, *Nat. Phys.* 5 (6) (2009) 438–442.
- [18] Karl Landsteiner, Yan Liu, Ya-Wen Sun, A quantum phase transition between a topological and a trivial semi-metal in holography (2015).
- [19] Rundong Li, Jing Wang, Xiao-Liang Qi, Shou-Cheng Zhang, Dynamical axion field in topological magnetic insulators, *Nat. Phys.* 6 (4) (2010) 284–288.
- [20] Heon-Jung Kim, Ki-Seok Kim, J-F. Wang, M. Sasaki, N. Satoh, A. Ohnishi, M. Kitaura, M. Yang, L. Li, Dirac versus Weyl fermions in topological insulators: Adler–Bell–Jackiw anomaly in transport phenomena, *Phys. Rev. Lett.* 111 (24) (2013) 246603.
- [21] Yeong-Chuan Kao, Mahiko Suzuki, Radiatively induced topological mass terms in (2 + 1)-dimensional gauge theories, *Phys. Rev. D* 31 (8) (1985) 2137.
- [22] Marc D. Bernstein, Taejin Lee, Radiative corrections to the topological mass in (2 + 1)-dimensional electrodynamics, *Phys. Rev. D* 32 (4) (1985) 1020.
- [23] Stefan Hohenegger, Ingo Kirsch, A note on the holography of Chern–Simons matter theories with flavour, *J. High Energy Phys.* 2009 (04) (2009) 129.
- [24] Mitsutoshi Fujita, Wei Li, Shinsei Ryu, Tadashi Takayanagi, Fractional quantum hall effect via holography: Chern–Simons, edge states and hierarchy, *J. High Energy Phys.* 2009 (06) (2009) 066.
- [25] Yoshinori Matsuo, Sang-Jin Sin, Shingo Takeuchi, Takuya Tsukioka, Chern–Simons term in holographic hydrodynamics of charged ads black hole, *J. High Energy Phys.* 2010 (4) (2010) 1.
- [26] Aristomenis Donos, Jerome P. Gauntlett, Christiana Pantelidou, Spatially modulated instabilities of magnetic black branes, *J. High Energy Phys.* 2012 (1) (2012) 1.
- [27] Shin Nakamura, Hiroshi Ooguri, Chang-Soon Park, Gravity dual of spatially modulated phase, *Phys. Rev. D* 81 (4) (2010) 044018.
- [28] Hiroshi Ooguri, Chang-Soon Park, Holographic endpoint of spatially modulated phase transition, *Phys. Rev. D* 82 (12) (2010) 126001.
- [29] Sophia K. Domokos, Jeffrey A. Harvey, Baryon-number-induced Chern–Simons couplings of vector and axial-vector mesons in holographic qcd, *Phys. Rev. Lett.* 99 (14) (2007).
- [30] Aristomenis Donos, Jerome P. Gauntlett, Holographic striped phases, *J. High Energy Phys.* 2011 (8) (2011) 1.
- [31] Oren Bergman, Niko Jokela, Gilad Lifshytz, Matthew Lippert, Striped instability of a holographic Fermi-like liquid, *J. High Energy Phys.* 2011 (10) (2011) 1.
- [32] Tomas Andrade, Benjamin Withers, A simple holographic model of momentum relaxation, *J. High Energy Phys.* 1405 (2014) 101.
- [33] Y. Kopelevich, P. Esquinazi, J.H.S. Torres, S. Moehlecke, Ferromagnetic- and superconducting-like behaviour of graphite, *J. Low Temp. Phys.* 119 (2000) 691.
- [34] L.D. Landau, L.P. Pitaevskii, E.M. Lifshitz, *Electrodynamics of Continuous Media, Course of Theoretical Physics*, vol. 8, 1984.
- [35] Keun-Young Kim, Kyung Kiu Kim, Yunseok Seo, Sang-Jin Sin, Coherent/incoherent metal transition in a holographic model, *J. High Energy Phys.* 1412 (2014) 170.
- [36] Mike Blake, Aristomenis Donos, Nakarin Lohitsiri, Magnetothermoelectric response from holography (2015).
- [37] Sean A. Hartnoll, Pavel Kovtun, Hall conductivity from dyonic black holes, *Phys. Rev. D* 76 (2007) 066001.
- [38] Naoto Nagaosa, Anomalous hall effect, *Rev. Mod. Phys.* 82 (2) (2010) 1539–1592.
- [39] Shigeki Onoda, Quantum transport theory of anomalous electric, thermoelectric, and thermal hall effects in ferromagnets, *Phys. Rev. E* 77 (16) (2008).
- [40] L. Berger, Side-jump mechanism for the hall effect of ferromagnets, *Phys. Rev. E* 2 (11) (1970) 4559.
- [41] J. Smit, The spontaneous hall effect in ferromagnetics i, *Physica* 21 (6) (1955) 877–887.
- [42] Jan Smit, The spontaneous hall effect in ferromagnetics ii, *Physica* 24 (1) (1958) 39–51.
- [43] N.R. Cooper, Thermoelectric response of an interacting two-dimensional electron gas in a quantizing magnetic field, *Phys. Rev. E* 55 (4) (1997) 2344–2359.